Journal of Cellular Biochemistry 102:453–462 (2007)

Constitutive Collagenase-1 Synthesis Through MAPK Pathways Is Mediated, in Part, by Endogenous IL-1α During Fibrotic Repair in Corneal Stroma

Jae-Chang Jung,[1]* Man-Il Huh,[1] and M. Elizabeth Fini[2]

[1]Department of Biology, College of Natural Sciences, Kyungpook National University, Daegu, Korea
[2]Evelyn F. and William L. McKnight Vision Research Center, Bascom Palmer Eye Institute, University of Miami Miller School of Medicine, Miami, Florida

Abstract Collagenase-1 is a protease expressed by active fibroblasts that is involved in remodeling of the extracellular matrix (ECM). In this study, we characterize the intracellular signaling mechanism of collagenase-1 production by IL-1α in subcultured normal fibroblasts (NF) from uninjured normal corneas, compared to that in repair wound fibroblasts (WF). In NF, collagenase-1 was induced specifically after the exogenous addition of IL-1α via activation of ERK and p38MAPK. Collagenase-1 expression was strongly suppressed upon treatment with either a MEK or p38MAPK inhibitor. In contrast, repair WF constitutively synthesized both IL-1α and collagenase-1. Combined treatment with both mitogen-activated protein kinase (MAPK) inhibitors dramatically reduced collagenase-1 synthesis, while individual MEK1 or p38 inhibitors weakly modulated the collagenase-1 level. The results indicate that both pathways are crucial in the regulation of collagenase-1 synthesis. Furthermore, an IL-1α receptor antagonist (IL-1ra) could not abolish constitutive collagenase-1 synthesis, even at high doses, suggesting that other cytokines/factors are additionally involved in this process. We propose that induction of collagenase-1 by IL-1α in both WF and NF depends on a unique combination of cell type-specific signaling pathways. J. Cell. Biochem. 102: 453–462, 2007.

Key words: collagenase-1; corneal stroma; fibrosis; MAPK; IL-1α

The cornea contains three layers, the outer squamous epithelium, inner endothelium, and central stroma containing quiescent stromal cells (keratocytes) embedded within a thick collagenous matrix. Upon ablation wounding, keratocytes located at the wound edge of the stroma begin to undergo mitosis along with morphological and functional changes, transform into active fibroblasts, and migrate into the damaged acellular area filled with fibrin clot [Weimar, 1962; Fini and Stramer, 2005]. Active fibroblasts synthesize new extracellular matrix (ECM) molecules distinct from normal uninjured stroma, as well as collagenase-1, which is not produced by keratocytes of normal corneas [Girard et al., 1993; Fini, 1999]. During the contraction phase of wound healing, fibroblasts transform into myofibroblasts expressing α-smooth muscle actin (α-SMA) that imparts contractile properties to cells [Jester et al., 1994; Jester et al., 1996]. Myofibroblasts generate abundant ECM, and participate in ECM remodeling by producing matrix metalloproteinases (MMPs) [Jain et al., 1996; Arthur, 1998; Ramadori et al., 1998]. In corneal wound healing, spontaneous fibroblast activation and myofibroblast transformation results in the deposition of opaque scar tissue, which interferes with vision [Fini and Stramer, 2005].

MMPs are zinc endopeptidases characterized by reactivity against all components of the ECM at neutral pH [Yong et al., 2001]. MMPs are subclassified into the following functional groups: collagenases, gelatinases, stromelysins, matrilysins, membrane type-MMPs (MT-MMPs), and

Grant sponsor: Korea Research Foundation; Grant number: R05-2003-000-11051-0; Grant sponsor: NIH; Grant number: R01 EY09828; Grant sponsor: Research to Prevent Blindness, Inc.

*Correspondence to: Jae-Chang Jung, PhD, Developmental Biology Laboratory, Department of Biology, College of Natural Sciences, Kyungpook National University, Daegu 702-701, Korea. E-mail: jcjung@mail.knu.ac.kr

Received 30 September 2006; Accepted 24 January 2007

DOI 10.1002/jcb.21309

other non-classified proteases [Visse and Nagase, 2003]. Transcription of MMP genes is controlled by a variety of cytokines, hormones, stress stimuli, and other environmental cues [Fini et al., 1998]. Furthermore, MMP activity is regulated by appropriate activators present in the extracellular space via a variety of proteolytic mechanisms in vivo [Girard et al., 1993; Lampert et al., 1998]. Collagenase-1 (MMP-1) cleaves native interstitial collagens. The denatured collagen triple helix is further degraded by other MMPs [Matsubara et al., 1991]. As a rule, resident cells synthesize collagenase-1 only upon demand for remodeling, such as early development and wound healing [Fini et al., 1998]. Abnormal MMPs have profound effects on the composition and organization of the ECM due to an imbalance between its synthesis and degradation, leading to pathological conditions, particularly tumor invasion, metastasis, ulceration, fibrosis, and arthritis [Matsubara et al., 1991; Fini, 1999]. Numerous diffusible cytokines and growth factors, including IL-1α and transforming growth factor-β (TGF-β), act as paracrine or autocrine mediators of collagenase-1 expression, depending on the tissue and cell type [Lyons et al., 1993; Fini et al., 1994; Reitamo et al., 1994; Sciavolino et al., 1994; Tamai et al., 1995; Tan et al., 1995; West-Mays et al., 1997].

The mechanisms of transcriptional and translational regulation of collagenase-1 have been investigated by treating sub-cultured cells isolated from normal corneas or cell lines that do not accurately reflect the healing tissue pattern of collagenase-1 regulation in vivo with various cytokines and reagents. Here, we reported the mitogen-activated protein kinase (MAPK) signaling pathways necessary for collagenase-1 production in response to IL-1α in vivo by using repair wound fibroblasts (WF) isolated from healing corneas and fibroblasts (NF) isolated from normal corneas.

MATERIALS AND METHODS

Penetrating Keratectomy (Ablation Wound)

Surgical procedures were performed in accordance with the ARVO statement for the use of animals in ophthalmic and vision research. A rabbit penetrating keratectomy model was used to study fibrotic repair [Cintron et al., 1973; Cintron et al., 1982; Girard et al., 1993; West-Mays et al., 1997]. Briefly, New Zealand white rabbits (3 kg) were anesthetized by intraperitoneal injection of tribromoethanol (Avertin; Aldrich, Milwaukee, WI). A 2 mm thick button of central corneal tissue comprising all three layers (epithelium, stroma, and endothelium) was ablated using a 2 mm trephine. The non-injured contralateral eye served as a control. Corneal wounds were allowed to heal for up to 20 days.

Morphological Examination

Wounded corneas from various time-points were processed for morphology by OCT (Tissue Tek, Elkhart, IN) embedding. Sections (7 μm thick) were fixed in 4% paraformaldehyde, and stained with Hematoxylin/Eosin and α-SMA. Images were captured on a fluorescence microscope equipped with a digital camera (Nikon, Tokyo, Japan).

Isolation of Stromal Cells and Culture

Twenty days after wound healing, animals were euthanized by lethal injection with sodium pentobarbital, and the corneas removed. The repair tissue occupying the original penetrating wound was isolated. Uninjured normal corneas of each rabbit were also removed using 7.2 mm trephine. Corneal stromal cells were isolated and cultured, as described previously [Fini and Girard, 1990; Fini, 1999]. Briefly, both epithelial and endothelial layers were gently scraped away with a scalpel after trypsin treatment of corneas at RT for 30 min. Stromal layers were further incubated with collagenase (5 mg/ml) at 37°C for 3 h to release stromal cells. For studies on primary cultures, cells were plated immediately after isolation. At confluence, cultures were removed from the dish with trypsin-EDTA, and split into three new culture dishes (first passage). The same passage numbers of NF and WF (between passages 1 and 5) were used.

Immunofluorescence and Phase-Contrast Microscopy

Freshly isolated repair WF were seeded at 1×10^4 cells per eight-chamber slide (Tissue-Tek; VWR Scientific) in MEM containing 10% FCS, and allowed to attach and spread overnight. For co-visualizing α-SMA and collagenase-1, the medium was removed, and the cell layer washed twice with PBS and fixed with 4% paraformaldehyde in PBS for 5 min. Cells were

permeabilized in 0.3% Triton X-100 for 2 min, and incubated with a monoclonal collagenase-1 antibody (DSHB, University of Iowa) at room temperature for 1 h. Cells were washed with PBS, and then incubated with the TRITC-conjugated goat anti-mouse antibody (Sigma–Aldrich, St. Louis, MO) for 1 h. After wash, cells were further incubated with the FITC-conjugated monoclonal α-SMA antibody (Sigma–Aldrich) at room temperature for 1 h. Prior to mounting, cells were washed three times with PBS. Images were captured on a Nikon fluorescence microscope.

Cell Treatment

Equal numbers (2×10^5 cells/well) of freshly isolated or sub-cultured cells were plated on 24-well cluster dishes in MEM medium containing 10% supplemented calf serum (FCS), and left to attach and spread on the dish overnight. The next day, the medium was replaced with a 300 μl of serum-free medium and treatment reagents. Experiments were performed in duplicate or triplicate to ensure reproducibility. To determine whether collagenase-1 synthesis is regulated by IL-1α, an IL-1 receptor antagonist (R & D Systems, Minneapolis, MN), IL-1ra (20, 100, and 500 ng/ml) was added to WF for 24 h. To induce collagenase-1 synthesis, NF were treated with human recombinant IL-lα (R & D Systems) (10 ng/ml). Cells were treated with 20 μM PD98059 (Calbiochem, San Diego, CA) or 20 μM SB203580 (Calbiochem) for 24 h in the presence or absence of IL-1α or IL-1ra (100 ng/ml) to analyze whether the ERK and p38MAPK pathways regulate collagenase-1 synthesis.

Preparation of Conditioned Media

The levels of secreted proteins were analyzed from equal numbers of cultured cells in serum-free medium for 24 h. Media were collected, and equal volumes of supernatant (usually 100 μl) were divided into aliquots. Secreted proteins in each aliquot were precipitated with a 10% ice-cold trichloroacetic acid (TCA). Precipitates were washed twice with 100% acetone to remove the remaining TCA. Air-dried precipitates were dissolved in a RIPA buffer, and stored at −20°C until use.

Western Blot Analysis

Western blot analysis was performed using standard techniques. Equal amounts of conditioned media or protein lysates (30 μg) in RIPA buffer were separated by 10% SDS–PAGE under non-reducing conditions, and the proteins transferred electrophoretically onto nitrocellulose membranes. Next, membranes were blocked in 5% non-fat dried milk in Tris-buffered saline containing 0.1% Tween-20 (TBS-T) for 1 h to minimize non-specific binding. Primary antibodies against collagenase-1, IL-1α (Endogen, Woburn, MA), phospho-ERK1/2 (New England Biolabs, Beverly, MA), and p38MAPK and phospho-p38MAPK (New England Biolabs) were diluted in TBS-T containing 5% dried milk (diluted 1: 2,000), and incubated for 1 h. Primary antibodies were detected by incubation with horseradish peroxidase (HRP)-conjugated secondary antibodies for a further 1 h. Specific antibody binding was visualized using the enhanced chemiluminescence detection kit (Amersham, Biosciences) with X-ray film exposure. Experiments were performed in triplicate.

Statistical Analysis

Data are presented as the mean ± SEM. The percentage of active fibroblasts and myofibroblasts from the primary cultured WF was evaluated by Student's t-test. $P < 0.0001$ was considered statistically significant.

RESULTS

Hypercellular and Fibrotic Repair Stroma

Following injury, the cornea becomes opaque during wound healing. This opacity becomes quite pronounced in a few h [Cintron et al., 1973; Cintron et al., 1982]. In our experiments, the central wound area was translucent, while the rest of the cornea remained intact after 3 days (Fig. 1A). Morphologically, only one cell layer of regenerating epithelium was observed across the wound region, and the stromal layer of the wound primarily constituted an acellular fibrin clot. By day 20 (Fig. 1B,C), the entire central stromal wound area was edematous and filled with numerous cells, as revealed by H&E staining. To establish whether myofibroblasts are present in fibrotic healing cornea, we stained for α-SMA, a specific myofibroblast marker. Interestingly, α-SMA-expressing myofibroblasts appeared mostly in the posterior region of hypercellular repair stroma (Fig. 1D).

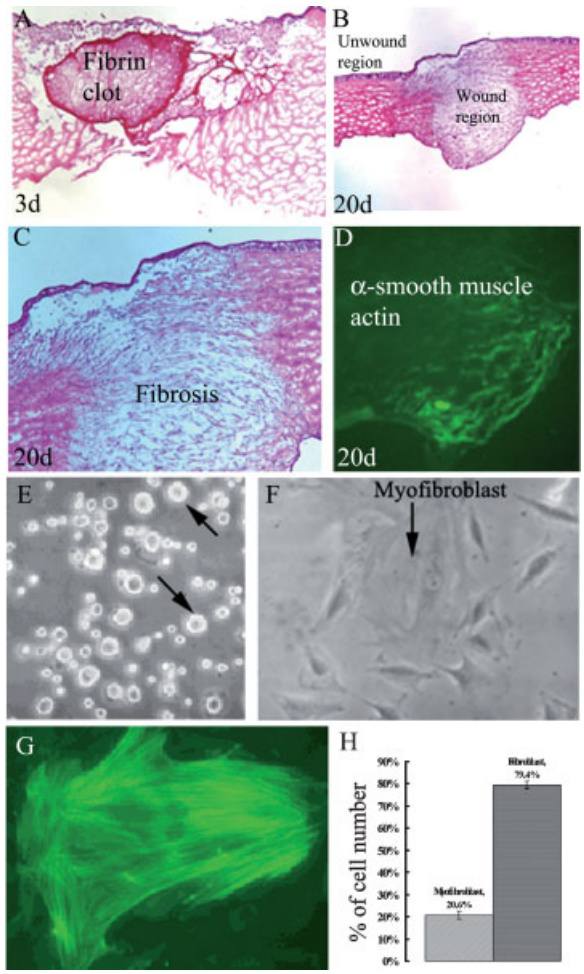

Fig. 1. Corneal stromal scar formation in ablation wounds and expression of α-SMA in cultured repair WF isolated from fibrotic healing corneas at day 20. **A**: At 3 days after wounding, the epithelium adjacent to the wound crossed along the fibrin clot surface. The ablated area is filled primarily with acellular fibrous stroma. **B**,**C**: In ablation wounds at day 20, the central stromal wound area contained numerous cells, and the scar progressively increased in opacity and appeared less edematous. **D**: Notably, significant α-SMA expression is detected in the posterior part of scar cornea by day 20. **E**: Freshly isolated stromal cells were examined at 30 min after plating. Phase-contrast microscopy reveals two heterogeneous cell sizes. **F**: At 2 h after plating, we observed bigger cells (arrows) identified as myofibroblasts, and smaller cells that were active fibroblasts. **G**: Following overnight culture, only bigger cells (cell number; $20.6 \pm 1.79\%$) stained for α-SMA (Higher magnification). **H**: Two hours after plating, bigger cells ($20.6 \pm 1.79\%$) and smaller cells ($79.4 \pm 1.79\%$) presumably represented myofibroblasts and active fibroblasts, respectively.

Wound Tissue Contains Fibroblasts and Myofibroblasts

To determine whether active fibroblasts and myofibroblasts are present in hypercellular situations during remodeling of corneal repair tissue, freshly isolated stromal cells at 20 days after wounding were subjected to primary culture. Phase-contrast microscopy revealed two heterogeneous cell sizes within 30 min after plating (Fig. 1E). A $20.6 \pm 1.79\%$ of bigger cells (arrows) and a $79.4 \pm 1.79\%$ of smaller cells presumably represented myofibroblasts and active fibroblasts 2 h after plating, respectively (Fig. 1E,F,H). Primary cultured stromal cells from uninjured normal cornea initially displayed round morphology due to unorganized cortical actin cytoskeleton until day 3 of culture in serum conditions [Jester et al., 1994; Fini, 1999]. In contrast, WF containing both active fibroblasts and myofibroblasts 2 h after plating developed a spindle shape and an organized actin cytoskeleton characteristic of wound healing. The next day, α-SMA-expressing myofibroblasts were examined by immunofluorescence microscopy. As expected, only bigger cells (cell number; $20.6 \pm 1.79\%$) expressed α-SMA (Fig. 1G; Higher magnification of myofibroblast).

Phase-contrast microscopy revealed a percentage of bigger myofibroblasts in patches at 2 days after WF culture (Fig. 2A). However, subcultured NF were negative for α-SMA (data not shown). Clearly, α-SMA staining is increased in successive subcultured WF, regardless of plating cell density (data not shown).

Collagenase-1 and IL-1α Synthesis in Primary Cultured WF

To examine whether the myofibroblasts or activate fibroblasts are synthesizing collagenase-1, immunofluroscence staining using primary cultured WF was performed (Fig. 2B). We found that both active fibroblasts and α-SMA-expressing myofibroblasts (green) expressed collagenase-1 (red).

Autocrine cytokine loops are activated in tissue repair, disease, and cellular aging, and serve as a mechanism for stimulating and maintaining the expression of specific genes [West-Mays et al., 1995; West-Mays et al., 1997; Cook et al., 1999]. We investigated whether IL-1α acts as an autocrine signal to maintain collagenase-1 expression in subcultured WF. IL-1α was strongly detected in the conditioned medium of subcultured WF, but barely in NF. Interestingly, both active (18 kDa) and precursor forms (≈ 33 and ≈ 31 kDa) of IL-1α were expressed in the conditioned media of WF (Fig. 2C). In contrast, only precursor IL-1α

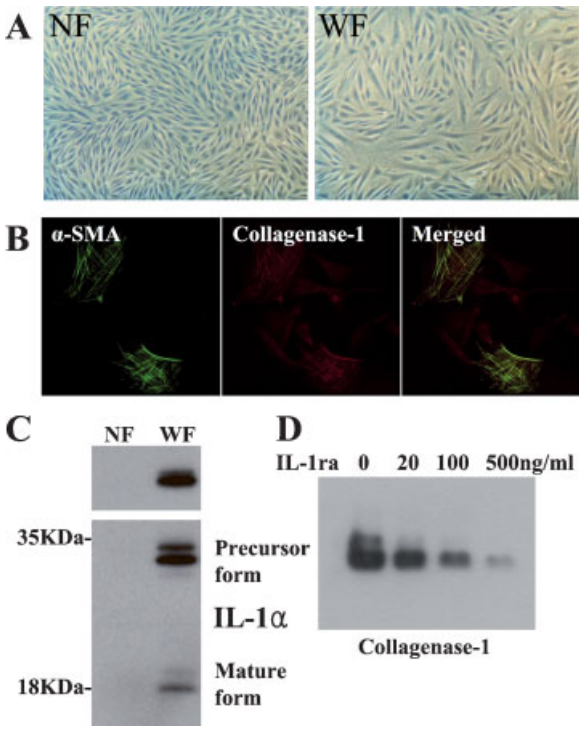

Fig. 2. High levels of collagenase-1 and IL-1α are constitutively expressed in primary cultured WF. **A**: Both NF and WF were grown to near confluence in MEM containing 10% FCS for 2 days. Phase-contrast microscopy revealed phenotypic differences between NF and WF. **B**: Primary cultured WF were immunostained with collagenase-1 (red) and a-SMA (green). Note that both cell types expressed collagenase-1. **C**: Equal numbers (5×10^4 cells/well) of freshly isolated NF and WF were plated in the presence of 10% serum overnight. Thereafter, cells were cultured in serum-free medium for 24 h. Western blot analysis of IL-1α secretion was performed using equal volumes of conditioned media. Both pro (≈33 and ≈31 kDa) and mature IL-1α (≈18 kDa) were strongly detected in WF, but not NF. **D**: Equal numbers (5×10^4 cells/well) of fleshly isolated WF were plated in the presence of 10% serum overnight. Thereafter, cells were cultured in serum-free medium in the presence of an IL-1ra (20, 100, and 500 ng/ml) for 24 h. Collagenase-1 synthesis using equal volumes of conditioned media was analyzed by Western blot. High levels of collagenase-1 (≈53 and ≈51 kDa) synthesis were greatly decreased by IL-1ra in a dose-dependent manner.

was detected in LPS-induced tear samples from the ulcerated eye [Schultz et al., 1997]. Both IL-1α forms actively bind to the IL-1 receptor [Mosley et al., 1987], and contribute to collagenase-1 expression.

To determine whether autocrine IL-1α controls collagenase-1 expression, primary cultured WF were treated with IL-1ra (20, 100, and 500 ng/ml), a naturally occurring analog of IL-1 that binds to its receptors but does not transduce a signal [Dinarello and Thompson, 1991]. After 24 h of culture, western blot analysis was performed on equal volumes of conditioned medium samples. As shown in Figure 2D, high levels of collagenase-1 (≈53 and ≈51 kDa) were synthesized in WF. As expected, IL-1ra dose-dependently inhibited collagenase-1 secretion of WF (Fig. 2D), since the analog competes with endogenous IL-1α for receptor binding and interferes with signal transduction [Wang et al., 2001].

Differential Involvement of the ERK and p38 Pathways in Collagenase-1 Synthesis in Both Cell Types

Collagenase-1 was not detectable in the conditioned media of subcultured NF (Fig. 3A), but its secretion was induced when cells were treated with exogenous IL-1α (10 ng/ml). By contrast, high levels of collagenase-1 were constitutively expressed in the WF by endogenous IL-1α (Fig. 2C and Fig. 3B). Interestingly, collagenase-1 was further stimulated by exogenous IL-1α in the WF (data not shown). It is

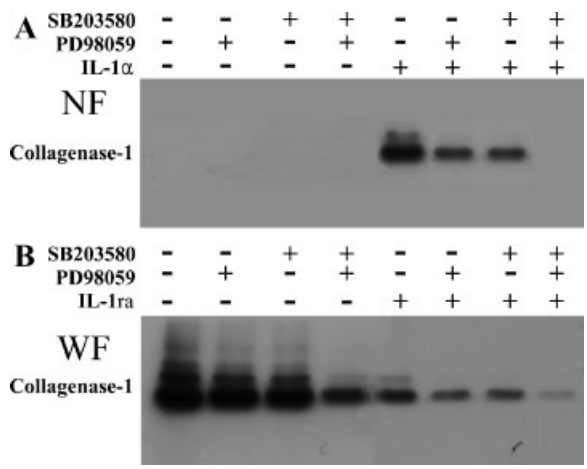

Fig. 3. Differences in the kinetic properties of regulation of collagenase-1 synthesis through MAPK signaling pathways in both cell types. Equal numbers (5×10^4 cells/well) of subcultured (3rd passage) NF and WF were serum-starved overnight, and treated with IL-1α (10 ng/ml) or IL-1ra (100 ng/ml) for 24 h in the presence or absence of MAPK inhibitors. Equal volumes of serum-free conditioned media from both cell types were precipitated with TCA, and dissolved proteins separated by 12% SDS–PAGE. **A**: The MEK inhibitor (20 μM PD98059) or p38 MAPK inhibitor (2 μM SB203580) reduced IL-1α mediated induction of collagenase-1 expression in NF, as revealed by immunoblotting. Combined treatment with both inhibitors completely abolished IL-1α-induced collagenase-1 synthesis in NF. **B**: In contrast, co-treatment with MEK and p38 MAPK inhibitors led to a dramatic suppression in collagenase-1 synthesis in WF, while individual MAPK inhibitors did not have a significant effect. Furthermore, collagenase-1 synthesis was not abrogated completely by IL-1ra in the presence of both MAPK inhibitors.

possible that exogenous IL-1α activates the IL-1α autocrine loop to synthesize more collagenase-1. MAPK pathways are implicated in the activation of collagenase-1 gene expression in other fibroblastic cells [Ridley et al., 1997; Reunanen et al., 1998; Vincenti et al., 1998; Westermarck et al., 1998]. To determine the individual MAPK pathways involved in collagenase-1 synthesis, both subcultured NF and WF were left untreated or stimulated with IL-1α in the absence and presence of specific MAPK inhibitors for 24 h. SB203580 is an inhibitor of p38 kinase, while PD98059 inhibits MEK1, the upstream activator of p44/p42 ERK kinases. As shown in Figure 3A, IL-1α-induced collagenase-1 synthesis was significantly decreased upon treatment with either PD98059 (20 μM) or SB203580 (20 μM) in NF. Collagenase-1 inhibition was dose-dependent (data not shown). However, combined treatment with both inhibitors completely abolished IL-1α-induced collagenase-1 synthesis, suggesting that the two pathways function in concert to induce collagenase-1. In WF (Fig. 3B), treatment with either PD98059 or SB203580 did not significantly affect the levels of constitutively expressed collagenase-1. Upon co-treatment with both inhibitors, collagenase-1 synthesis in WF was significantly reduced. Interestingly, collagenase-1 synthesis was not completely abolished by IL-1ra treatment (100 ng/ml) in the presence of both MAPK inhibitors. The data suggest that other unknown factors or pathways in WF are additionally involved in the regulation of collagenase-1 synthesis.

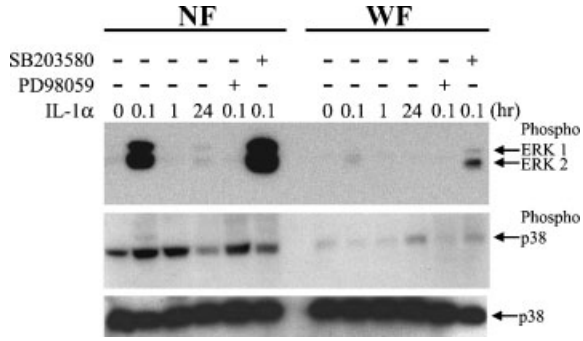

Fig. 4. Differential activation of ERK 1/2 and p38MAPK in both cell types. Equal numbers of sub-cultured (passage 4) NF and WF were serum-starved for 24 h, and treated directly with IL-1α without changing the medium for 10 min, 1 h, and 24 h. Cells were lysed, fractionated by 10% SDS–PAGE, and active phosphorylated proteins detected by immunoblot analysis. IL-1α treatment resulted in rapid and transient activation of both ERK1 and ERK2 in NF, as indicated by the appearance of dually phosphorylated forms of kinases within 10 min. Kinase activities were abrogated within 1 h. Pre-treatment of NF with PD98059 for 30 min blocked IL-1α-induced activation of both ERK1 and ERK2. Interestingly, inhibition of the p38 pathway by pre-treatment with SB203580 in NF stimulated IL-1α-induced activation of both ERK1 and ERK2. A high basal level of phosphorylated p38MAPK was detected in untreated NF. Phosphorylated p38MAPK between 10 min and 1 h was stimulated by IL-1α, but was decreased by 24 h after treatment. Pre-treatment of cells with SB203580 partially inhibited IL-1α-induced activation of p38MAPK, while PD98059 applied before IL-1α treatment did not affect p38MAPK. On the other hand, transient activation of both ERK and p38MAPK was dramatically downregulated by a continuous IL-1α signal that was expressed constitutively in WF during serum starvation. Similar patterns of MAPK activation were observed in both cell types upon treatment with IL-1α only in fresh serum-free medium after serum starvation. P38 was used as a loading control. The data are representative of three independent experiments.

Transient Activation of ERK and p38MAPK Pathways by IL-1α in NF, but Not WF

To establish whether the ERK and p38MAPK pathways are required for collagenase-1 synthesis, subcultured NF and WF were serum-starved for 24 h, and left untreated or treated with IL-1α. Cells were harvested at various time-points, and equal amounts of protein assayed by Western blotting using antibodies specific for the phosphorylated and active forms of ERK and p38MAPK. As shown in Figure 4, IL-1α treatment resulted in the rapid and transient activation of both ERK1 and ERK2, as evident from the appearance of the dually phosphorylated forms of these kinases within 10 min. Neither band was detected at 1 h. To determine whether PD98059 blocked ERK activation, NF were pre-treated with the MEK1 inhibitor for 30 min, followed by IL-1α treatment for 10 min. As expected, PD98059 completely abolished IL-1α-induced activation of the ERK pathway, since MEK1 is the upstream activating kinase of ERK1 and ERK2. On the other hand, pre-treatment of cells with SB203580 for 30 min before IL-1α treatment significantly stimulated activation of the ERK pathway (Fig. 4). Constitutive and strong p38MAPK activation was observed in untreated NF (Fig. 4). Phosphorylation of p38MAPK by IL-1α was increased between 10 min and 1 h, but decreased by 24 h after treatment. To determine whether SB203580 inhibits p38MAPK activation, NF were pre-treated with SB203580 for 30 min, followed by IL-1α treatment for 10 min.

While SB203580 inhibited partially IL-1α-induced activation of p38MAPK, the p38 pathway was not affected by PD98059 applied for 30 min before IL-1α treatment.

In WF, the ERK pathway was barely activated after IL-1α treatment for 10 min, but was not detected following pre-treatment with PD98059 before the addition of IL-1α (Fig. 4). However, application of SB203580 to WF for 30 min before IL-1α treatment for 10 min stimulated the ERK pathway to a minor extent. Phosphorylated p38MAPK was detected in untreated WF, but its level was weaker than that in NF. Activation of p38MAPK by IL-1α was not affected between 10 min and 1 h, but was slightly increased by 24 h after treatment. Compared to ERK, p38MAPK activation was merely changed when cells were pre-treated for 30 min with either SB203580 or PD98059 before IL-1α treatment for 10 min. The data collectively demonstrate that both ERK and p38 pathways are transiently stimulated by exogenous IL-1α in NF, but not WF, possibly due to the high levels of endogenous IL-1α already activated under these conditions. Furthermore, inhibition of the p38 pathway triggered ERK signaling in both NF and WF, suggesting crosstalk between MEK-ERK and p38MAPK that is specific to IL-1α stimulation.

DISCUSSION

The cornea provides a unique model for examining wound healing processes due to its simple structure. With the recent increase in vision corrective surgeries that reshape the corneal stroma, understanding the stromal cell repair pathway is of vital importance. In contrast to skin, no cellular appendages are present in the stromal layer of cornea. Therefore, pure populations of stromal cells can be isolated from uninjured normal corneas and cultured with ease. In this study, we investigate the presence of fibroblasts and myofibroblasts in the repairing stroma in vivo, as well as in vitro. Interestingly, we observed mixed cell populations of stromal cells with different cell sizes and shapes, as well as α-SMA staining patterns, in primary cultured repair WF (Fig. 1E–G), suggesting that morphological changes correlate with the wound healing process. Reports in the pre- "regenerative medicine" era literature implicated "wandering cells" in wound healing. However until a few years ago, it had become generally accepted that corneal stromal keratocytes were the sole source of wound fibroblasts and myofibroblasts. Now, there is increasing new evidence that keratocytes that "wandering" bone marrow-derived cells are likely to contribute in some way [Nakamura et al., 2005]. Nevertheless, keratocytes are still clearly the important players in corneal wound repair. In cultured WF, myofibroblasts contain more stress fibers and focal adhesions than other fibroblasts [Jester et al., 1994; Fini, 1999]. The morphology of these cells suggests a transition between fibroblasts and myofibroblasts. Transition of the fibroblast phenotype in repair tissue is a developmental event, which reflects changes in the hard wiring of signaling pathways by which the cell responds to environmental input [Fini, 1999].

Within 3 weeks, the fibrin clot was largely replaced by repair WF (Fig. 1C). Alteration of the actin cytoskeleton occurs during numerous remodeling situations in vivo, such as cell migration and wound contraction [Fini et al., 1998; Stramer et al., 2003]. During the contraction phase of corneal wound healing (Fig. 1), further differentiation of fibroblasts occurs as individual cells begin to acquire the "myofibroblast phenotype" characterized by expression of α-SMA that helps to impart contractile properties to the cells [Jester et al., 1994; Jester et al., 1996]. However, cell motility is inhibited [Ronnov-Jessen and Petersen, 1996].

Differentially expressed cytokines in normal and healing corneas may positively or negatively control aspects of the repair phenotype [Wilson et al., 1992; Wilson et al., 1994; Wilson et al., 2001]. Subcultured NF typically contains a percentage of myofibroblasts, probably due to the presence of TGF-β in serum used for culture. Addition of TGF-β to cultured cells induces further differentiation [Jester et al., 1996]. Masur et al. showed that this response is cell density-dependent [Masur et al., 1996]. Specifically, cells plated at a high density could not differentiate in response to serum or exogenously added TGF-β, while most cells plated at very low density differentiated into myofibroblasts within a week. In contrast to TGF-β-induced myofibroblast transformation in low-density cultures of NF in vitro [Masur et al., 1996], high-density cultures of WF mimic hypercellular situations, as evident from the morphology (Fig. 1), resulting in a fibrotic situation.

Both temporally and spatially expressed cytokines and growth factors including IL-1α and TGF-β are identified across the sites of tissue remodeling in vivo, and may differentially modulate collagenase-1 as well as ECM expression [Girard et al., 1991; Fini et al., 1994; West-Mays et al., 1995; West-Mays et al., 1999]. We mainly focused on collagenase-1, which is specifically reactive against native type I and type V collagen, the major components of collagenous lamellae of the stroma that function in corneal transparency [Fitch et al., 1988; Birk et al., 1990]. Collagenase-1 gene expression is induced by UV light exposure and in multiple sub-cultured cells through the autocrine IL-1α loop [Kumar et al., 1992; Petersen et al., 1992]. The IL-1α autocrine feedback loop is absolutely required as an intermediate for the induction of collagenase-1 in NF [Fini et al., 1994; West-Mays et al., 1995; West-Mays et al., 1999]. Previously, West-Mays et al. could not detect active or precursor forms of IL-1α in WF using an enzyme-amplified sensitivity immunoassay [West-Mays et al., 1997]. In contrast, we observed high levels of both active and precursor endogenous IL-1α in conditioned WF media (Fig. 2C). Although IL-1ra was effective significantly in suppressing the collagenase-1 in the presence of both ERK and p38MAPK inhibitors in WF (Fig. 3B), but did not completely block its synthesis. Evidently other additional unknown factors and mechanisms, independent of IL-1α and MAPK pathways, are involved in the regulation of collagenase-1 expression in WF. One unique finding is that collagenase-1 can be induced or decreased in cultures of NF by IL-1α stimulation or WF by IL-1ra treatment, respectively (Fig. 3), suggesting that a form of this cytokine is an intermediate factor that regulates constitutive collagenase-1 expression. Fibrotic tissue fails to return to the native structure, since it is composed of a haphazard array of collagen fibrils and cellular elements that fill in and seal the injured area [Cintron et al., 1973; Cintron et al., 1982; Deuel et al., 1991]. Our data collectively suggest that collagenase-1 expression is mediated, at least in part, by endogenous IL-1α, and participates in the regulation of ECM remodeling associated with fibrosis formation.

The signaling mechanisms regulating collagenase-1 expression in repair WF remain to be established. In our experiments, the effects of IL-1α on MAPK activation are similar to those of HGF in corneal epithelial cells [Liang et al., 1998]. Interestingly, IL-1α- induced ERK activation at early time-points was facilitated by inhibition of the p38MAPK pathway in both NF and WF (Fig. 4), signifying p38MAPK-mediated modulation of ERK activation in response to IL-1α. In contrast, inhibition of MEK1 did not influence p38MAPK activation, confirming the specificity and unidirectionality of p38MAPK-ERK crosstalk in keeping with previous reports [Lewthwaite et al., 2006]. Our present in vitro studies show that the MEK-ERK and p38MAPK pathways in WF play similar roles in ECM remodeling of fibrotic wound repair by stimulating collagenase-1 via the IL-1α autocrine feedback loop.

Based on the results, we propose that IL-1α produced in an autocrine manner from corneal WF plays a crucial role in the remodeling of corneal fibrosis through ERK and p38MAPK pathways to regulate collagenase-1 expression. Elucidation of the molecular mechanisms controlling the MAPK pathways for collagenase-1 synthesis during wound healing may have wide applications in alleviating fibrosis in the eye due to surgical complications or pathological conditions, as well as other organs.

ACKNOWLEDGMENTS

This work was supported by a Korean Research Foundation Grant (R05-2003-000-11051-0), NIH R01 EY09828 (MEF) and P30 EY14801; Research to Prevent Blindness unrestricted (Tufts and Miami), Stein Professorship, and Senior Scientific Investigator; Walter G. Ross Chair in Ophthalmic Research.

REFERENCES

Arthur MJ. 1998. Fibrosis and altered matrix degradation. Digestion 59:376–380.

Birk DE, Fitch JM, Babiarz JP, Doane KJ, Linsenmayer TF. 1990. Collagen fibrillogenesis in vitro: Interaction of types I and V collagen regulates fibril diameter. J Cell Sci 95(Pt 4):649–657.

Cintron C, Schneider H, Kublin C. 1973. Corneal scar formation. Exp Eye Res 17:251–259.

Cintron C, Szamier RB, Hassinger LC, Kublin CL. 1982. Scanning electron microscopy of rabbit corneal scars. Invest Ophthalmol Vis Sci 23:50–63.

Cook JR, Mody MK, Fini ME. 1999. Failure to activate transcription factor NF-kappaB in corneal stromal cells (keratocytes). Invest Ophthalmol Vis Sci 40:3122–3131.

Deuel TF, Kawahara RS, Mustoe TA, Pierce AF. 1991. Growth factors and wound healing: Platelet-derived

growth factor as a model cytokine. Annu Rev Med 42: 567–584.
Dinarello CA, Thompson RC. 1991. Blocking IL-1: Interleukin 1 receptor antagonist in vivo and in vitro. Immunol Today 12:404–410.
Fini ME. 1999. Keratocyte and fibroblast phenotypes in the repairing cornea. Prog Retin Eye Res 18:529–551.
Fini ME, Girard MT. 1990. The pattern of metalloproteinase expression by corneal fibroblasts is altered by passage in cell culture. J Cell Sci 97(Pt 2):373–383.
Fini ME, Stramer BM. 2005. How the cornea heals: Cornea-specific repair mechanisms affecting surgical outcomes. Cornea 24:S2–S11.
Fini ME, Strissel KJ, Girard MT, Mays JW, Rinehart WB. 1994. Interleukin 1 alpha mediates collagenase synthesis stimulated by phorbol 12-myristate 13-acetate. J Biol Chem 269:11291–11298.
Fini ME, Cook JR, Mohan R, Brinckerhoff CE. 1998. Regluation of matrix metalloproteinase gene expression. In: Parks WC, Mecham RP, editors. Matrix metalloproteinases. New York: Academic Press. pp 299–356.
Fitch JM, Birk DE, Mentzer A, Hasty KA, Mainardi C, Linsenmayer TF. 1988. Corneal collagen fibrils: Dissection with specific collagenases and monoclonal antibodies. Invest Ophthalmol Vis Sci 29:1125–1136.
Girard MT, Matsubara M, Fini ME. 1991. Transforming growth factor-beta and interleukin-1 modulate metalloproteinase expression by corneal stromal cells. Invest Ophthalmol Vis Sci 32:2441–2454.
Girard MT, Matsubara M, Kublin C, Tessier MJ, Cintron C, Fini ME. 1993. Stromal fibroblasts synthesize collagenase and stromelysin during long-term tissue remodeling. J Cell Sci 104(Pt 4):1001–1011.
Jain M, He Q, Lee WS, Kashiki S, Foster LC, Tsai JC, Lee ME, Haber E. 1996. Role of CD44 in the reaction of vascular smooth muscle cells to arterial wall injury. J Clin Invest 97:596–603.
Jester JV, Barry PA, Lind GJ, Petroll WM, Garana R, Cavanagh HD. 1994. Corneal keratocytes: In situ and in vitro organization of cytoskeletal contractile proteins. Invest Ophthalmol Vis Sci 35:730–743.
Jester JV, Barry-Lane PA, Cavanagh HD, Petroll WM. 1996. Induction of alpha-smooth muscle actin expression and myofibroblast transformation in cultured corneal keratocytes. Cornea 15:505–516.
Kumar S, Millis AJ, Baglioni C. 1992. Expression of interleukin 1-inducible genes and production of interleukin 1 by aging human fibroblasts. Proc Natl Acad Sci USA 89:4683–4687.
Lampert K, Machein U, Machein MR, Conca W, Peter HH, Volk B. 1998. Expression of matrix metalloproteinases and their tissue inhibitors in human brain tumors. Am J Pathol 153:429–437.
Lewthwaite JC, Bastow ER, Lamb KJ, Blenis J, Wheeler-Jones CP, Pitsillides AA. 2006. A specific mechanomodulatory role for p38 MAPK in embryonic joint articular surface cell MEK-ERK pathway regulation. J Biol Chem 281:11011–11018.
Liang Q, Mohan RR, Chen L, Wilson SE. 1998. Signaling by HGF and KGF in corneal epithelial cells: Ras/MAP kinase and Jak-STAT pathways. Invest Ophthalmol Vis Sci 39:1329–1338.
Lyons JG, Birkedal-Hansen B, Pierson MC, Whitelock JM, Birkedal-Hansen H. 1993. Interleukin-1 beta and transforming growth factor-alpha/epidermal growth factor induce expression of M(r) 95,000 type IV collagenase/gelatinase and interstitial fibroblast-type collagenase by rat mucosal keratinocytes. J Biol Chem 268:19143–19151.
Masur SK, Dewal HS, Dinh TT, Erenburg I, Petridou S. 1996. Myofibroblasts differentiate from fibroblasts when plated at low density. Proc Natl Acad Sci USA 93:4219–4223.
Matsubara M, Zieske JD, Fini ME. 1991. Mechanism of basement membrane dissolution preceding corneal ulceration. Invest Ophthalmol Vis Sci 32:3221–3237.
Mosley B, Urdal DL, Prickett KS, Larsen A, Cosman D, Conlon PJ, Gillis S, Dower SK. 1987. The interleukin-1 receptor binds the human interleukin-1 alpha precursor but not the interleukin-1 beta precursor. J Biol Chem 262:2941–2944.
Nakamura T, Ishikawa F, Sonoda KH, Hisatomi T, Qiao H, Yamada J, Fukata M, Ishibashi T, Harada M, Kinoshita S. 2005. Characterization and distribution of bone marrow-derived cells in mouse cornea. Invest Ophthalmol Vis Sci 46:497–503.
Petersen MJ, Hansen C, Craig S. 1992. Ultraviolet A irradiation stimulates collagenase production in cultured human fibroblasts. J Invest Dermatol 99:440–444.
Ramadori G, Knittel T, Saile B. 1998. Fibrosis and altered matrix synthesis. Digestion 59:372–375.
Reitamo S, Remitz A, Tamai K, Uitto J. 1994. Interleukin-10 modulates type I collagen and matrix metalloprotease gene expression in cultured human skin fibroblasts. J Clin Invest 94:2489–2492.
Reunanen N, Westermarck J, Hakkinen L, Holmstrom TH, Elo I, Eriksson JE, Kahari VM. 1998. Enhancement of fibroblast collagenase (matrix metalloproteinase-1) gene expression by ceramide is mediated by extracellular signal-regulated and stress-activated protein kinase pathways. J Biol Chem 273:5137–5145.
Ridley SH, Sarsfield SJ, Lee JC, Bigg HF, Cawston TE, Taylor DJ, DeWitt DL, Saklatvala J. 1997. Actions of IL-1 are selectively controlled by p38 mitogen-activated protein kinase: Regulation of prostaglandin H synthase-2, metalloproteinases, and IL-6 at different levels. J Immunol 158:3165–3173.
Ronnov-Jessen L, Petersen OW. 1996. A function for filamentous alpha-smooth muscle actin: Retardation of motility in fibroblasts. J Cell Biol 134:67–80.
Schultz CL, Morck DW, McKay SG, Olson ME, Buret A. 1997. Lipopolysaccharide induced acute red eye and corneal ulcers. Exp Eye Res 64:3–9.
Sciavolino PJ, Lee TH, Vilcek J. 1994. Interferon-beta induces metalloproteinase mRNA expression in human fibroblasts. Role of activator protein-1. J Biol Chem 269: 21627–21634.
Stramer BM, Zieske JD, Jung JC, Austin JS, Fini ME. 2003. Molecular mechanisms controlling the fibrotic repair phenotype in cornea: Implications for surgical outcomes. Invest Ophthalmol Vis Sci 44:4237–4246.
Tamai K, Ishikawa H, Mauviel A, Uitto J. 1995. Interferon-gamma coordinately upregulates matrix metalloprotease (MMP)-1 and MMP-3, but not tissue inhibitor of metalloproteases (TIMP), expression in cultured keratinocytes. J Invest Dermatol 104:384–390.
Tan EM, Qin H, Kennedy SH, Rouda S, Fox JWt, Moore JH, Jr. 1995. Platelet-derived growth factors-AA and -BB

regulate collagen and collagenase gene expression differentially in human fibroblasts. Biochem J 310(Pt 2):585–588.

Vincenti MP, Schroen DJ, Coon CI, Brinckerhoff CE. 1998. v-src activation of the collagenase-1 (matrix metalloproteinase-1) promoter through PEA3 and STAT: Requirement of extracellular signal-regulated kinases and inhibition by retinoic acid receptors. Mol Carcinog 21: 194–204.

Visse R, Nagase H. 2003. Matrix metalloproteinases and tissue inhibitors of metalloproteinases: Structure, function, and biochemistry. Circ Res 92:827–839.

Wang N, Chintala SK, Fini ME, Schuman JS. 2001. Activation of a tissue-specific stress response in the aqueous outflow pathway of the eye defines the glaucoma disease phenotype. Nat Med 7:304–309.

Weimar V. 1962. Effect of amino acid, purine, and pyrimidine analogues on activation of corneal stromal cells to take up neutral red. Invest Ophthalmol 1:226–232.

Westermarck J, Holmstrom T, Ahonen M, Eriksson JE, Kahari VM. 1998. Enhancement of fibroblast collagenase-1 (MMP-1) gene expression by tumor promoter okadaic acid is mediated by stress-activated protein kinases Jun N-terminal kinase and p38. Matrix Biol 17: 547–557.

West-Mays JA, Strissel KJ, Sadow PM, Fini ME. 1995. Competence for collagenase gene expression by tissue fibroblasts requires activation of an interleukin 1 alpha autocrine loop. Proc Natl Acad Sci USA 92:6768–6772.

West-Mays JA, Sadow PM, Tobin TW, Strissel KJ, Cintron C, Fini ME. 1997. Repair phenotype in corneal fibroblasts is controlled by an interleukin-1 alpha autocrine feedback loop. Invest Ophthalmol Vis Sci 38:1367–1379.

West-Mays JA, Cook JR, Sadow PM, Mullady DK, Bargagna-Mohan P, Strissel KJ, Fini ME. 1999. Differential inhibition of collagenase and interleukin-1alpha gene expression in cultured corneal fibroblasts by TGF-beta, dexamethasone, and retinoic acid. Invest Ophthalmol Vis Sci 40:887–896.

Wilson SE, He YG, Lloyd SA. 1992. EGF, EGF receptor, basic FGF, TGF beta-1, and IL-1 alpha mRNA in human corneal epithelial cells and stromal fibroblasts. Invest Ophthalmol Vis Sci 33:1756–1765.

Wilson SE, Schultz GS, Chegini N, Weng J, He YG. 1994. Epidermal growth factor, transforming growth factor alpha, transforming growth factor beta, acidic fibroblast growth factor, basic fibroblast growth factor, and interleukin-1 proteins in the cornea. Exp Eye Res 59:63–71.

Wilson SE, Mohan RR, Mohan RR, Ambrosio R, Jr., Hong J, Lee J. 2001. The corneal wound healing response: Cytokine-mediated interaction of the epithelium, stroma, and inflammatory cells. Prog Retin Eye Res 20:625–637.

Yong VW, Power C, Forsyth P, Edwards DR. 2001. Metalloproteinases in biology and pathology of the nervous system. Nat Rev Neurosci 2:502–511.